Piezoresistive Effect of p-Type Single Crystalline 3C-SiC Thin Film

Hoang-Phuong Phan, Philip Tanner, Dzung Viet Dao, Li Wang, Nam-Trung Nguyen, Yong Zhu, and Sima Dimitrijev

***Abstract*— This letter presents for the first time the piezoresistive effect of p-type single crystalline 3C-SiC thin film. The 3C-SiC thin film was epitaxially grown on (100) p-type Si substrate using the low-pressure chemical vapor deposition (LPVCD) process. The grown 3C-SiC was doped *in situ* with aluminum to form p-type semiconductor with carrier concentration of 5×10^{18} cm^{-3} and sheet resistance of about 40 kΩ/□. Longitudinal and transverse gauge factors (GFs) of the 3C-SiC in [110] orientation at room temperature (23 °C) were 30.3 and −25.1, respectively. These results indicated that the p-type single crystalline 3C-SiC possessed a higher GF than the previously reported results in p-type polycrystalline 3C-SiC.**

***Index Terms*— Silicon carbide, piezoresistive effect, MEMS, 3C-SiC, p-type semiconductor.**

I. Introduction

THE Piezoresistive Effect in silicon (Si) has been widely applied in MEMS (Micro Electro Mechanical Systems) sensors thanks to its large gauge factor, miniaturization and electronics integration capability [1]–[3]. However, the drawbacks of the low energy band gap limited Si from operating at high temperature conditions. Recently, many researches have been focusing on large band gap materials for applications used in harsh environment. Among these materials, silicon carbide (SiC) is one of the most promising candidates due to its excellent mechanical and electrical properties [4]. There are more than two hundred poly-types of SiC crystal (eg. 3C, 4H, 6H-SiC) and studies on the piezoresistive effect of these poly-types have been proposed since two decades ago [5]–[7]. Akiyama *et al.* investigated the highly doped n-type 4H-SiC piezoresistor with the gauge factor (GF) of 20.8 [6]. Okojie *et al.* reported the GF of n-type and p-type 6H-SiC to be 22 and 27, respectively [8]. Compared to the hexagonal polytypes, the cubic crystal SiC (3C-SiC) attracts a great deal of interest for MEMS applications, since it can be grown directly on a Si substrate [9]. Shor *et al.* measured the piezoresistive coefficient of n-type single 3C-SiC grown by atmospheric pressure chemical vapor deposition (APCVD). The longitudinal GF in [100] direction at room temperature were −31.8, −26.6 and −12.7 for unintentional, lightly and degenerated dopes, respectively [10]. Eickhoff *et al.* investigated the dependence of piezoresisitive effect on crystal types of n-type 3C-SiC grown by LPCVD with the largest negative GF found in single crystal while poly and nano-crystals offered smaller GFs [11]. Numerous mechanical sensors have been developed based on the piezoresistive effect in 3C-SiC [10]–[13].

Most previous studies have focused on investigating n-type 3C-SiC. Little research has characterized the piezoresistive effect of p-type polycrystalline 3C-SiC with the GF of about 2∼8, and the piezoresistive characteristics of p-type single crystalline 3C-SiC have not been fully understood [14]. The work on p-type 3C-SiC piezoresistive effect is still limited due to the high temperature of growing process at around 1350 °C, which is close to Si melting point, affecting the dopant redistribution in Si, and accumulating the thermal mismatch between SiC and Si [15].

This letter reports, for the first time, the piezoresistive effect of p-type single crystalline 3C-SiC grown by using the LPCVD process at the low temperature of 1000 °C and in-situ doping. The longitudinal and transverse gauge factors in [110] direction were characterized. The shear piezoresistive coefficient π_{44} was calculated based on measured longitudinal and transverse GFs.

II. Device Fabrication

A. Growth Process of 3C-SiC on Si

The 3C-SiC was grown on Si(100) substrate by using a hot-wall LPCVD reactor at 1000 °C [15], [16]. The alternating supply epitaxy approach was used to achieve single crystalline SiC film deposition with silane (SiH_4) and propylene (C_3H_6) as precursors. Trimethylaluminium [$(CH_3)_3Al$, TMAl] was employed as p-type dopant. The AFM image of 280nm 3C-SiC is shown in Fig. 1(a) in which the roughness of $5\mu m \times 5\mu m$ area was 20nm. The full-range 2θ-ω scan from x-ray diffraction (XRD) measurement indicated that the SiC film is epitaxially grown on Si(100) substrate [as shown in Fig. 1(b)]. The electrical properties of SiC were determined by a hot probe and Hall Effect. The polarity of the hot probe voltage indicated that SiC was p-type conductivity. At room temperature the carrier concentration of p-type SiC was found to be 5×10^{18}cm^{-3}.

B. Fabrication of 3C-SiC on Si Beam

After SiC was grown on Si substrate by the LPCVD process (step 1), the SiC was then dry etched in an inductively coupled plasma etcher through to the Si substrate after patterning by standard photolithography techniques (step 2)

Manuscript received November 27, 2013; revised January 6, 2014; accepted January 15, 2014. Date of publication February 3, 2014; date of current version February 20, 2014. This work was supported by the Queensland node of the Australian National Fabrication Facility, a company established under the National Collaborative Research Infrastructure Strategy to provide nano and micro-fabrication facilities for Australia's researchers. The review of this letter was arranged by Editor M. Tabib-Azar.

The authors are with the Queensland Micro-Nanotechnology Centre, Griffith University, Nathan QLD 4111, Australia (e-mail: hoangphuong.phan@griffithuni.edu.au).

Color versions of one or more of the figures in this letter are available online at http://ieeexplore.ieee.org.

Digital Object Identifier 10.1109/LED.2014.2301673

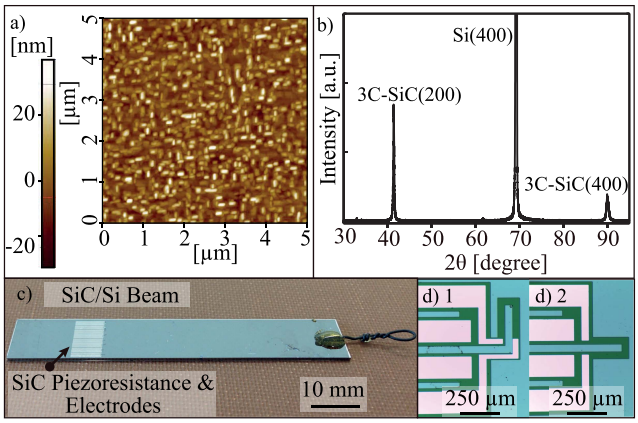

Fig. 1. Photographs of fabricated device. (a) AFM photograph of 3C-SiC; (b) XRD graph of growth 3C-SiC; (c) photograph of 3C-SiC beam; (d1) and (d2) transverse and longitudinal 3C-SiC resistors.

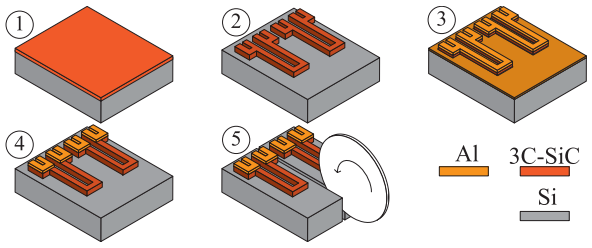

Fig. 2. Fabrication process of 3C-SiC/Si beam.

(Fig. 2). Two contact pads were connected to each end of the piezoresistor, so that four-point measurements could be performed to eliminate contact resistance from the measurement. Aluminium contacts were then sputtered (step3) and patterned to form electrodes on the SiC (step 4). The Si was then diced to form a strip 60mm×9mm×0.625mm [step5, Fig. 1(c)]. In order to measure longitudinal and transverse GFs, SiC resistors were arranged in [110] and [1$\bar{1}$0] directions [Fig. 1(d1) and (d2)]. The dimensions of the SiC resistors were 550μm×50μm×0.280μm for the short SiC resistor, and 1050μm×50μm×0.280μm for the long SiC resistor.

C. IV Curve of p-Type 3C-SiC/p-Type Si Heterojunction

As the p-type SiC ($N_a = 5 \times 10^{18}$cm^{-3}) was grown on the p-type Si ($N_a = 5 \times 10^{14}$cm^{-3}), the issue of current leakage through the SiC/Si junction was investigated to ensure that the Si substrate did not contribute to the measured piezoresistance. Due to the large valence band discontinuity between 3C-SiC (Ev = 6.9eV) and Si (Ev = 5.2eV), holes are blocked from flowing across the junction. This is particularly so when the SiC is positively biased with respect to the Si, resulting in an increased depletion. The current flow through SiC/Si junction was measured by sweeping voltage of SiC with respect to Si from −2V to 2V using an HP 4145B Analyzer. At negative voltage, the current increased with applied voltage more than 200mV, causing large current leaking through SiC/Si junction. At positive voltage, the current was considerably smaller, being 2.5nA at the supplied voltage of +0.5V (Fig. 3, left side). Therefore, to measure the resistance change of the SiC resistor, positive voltage was applied to the SiC

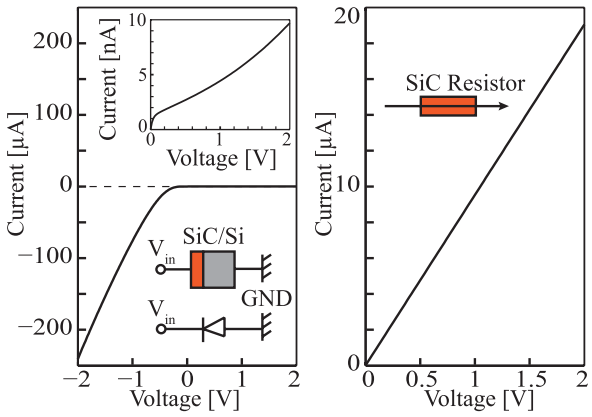

Fig. 3. I-V curves. On the left: current leakage through p-type SiC/p-type Si junction (small graph: zoom in of the current at positive voltage). On the right: I-V curve of SiC resistor.

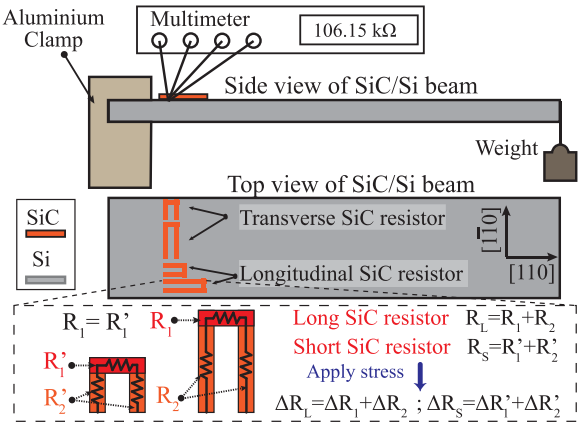

Fig. 4. Experimental setup. Side view: SiC/Si beam was clamped, and then bent by weights. Top view: SiC/Si beam with the SiC resistor arranged in [110] and [110] directions. Each SiC resistor consisted of 2 sections: longitudinal SiC resistor R_2 and transverse SiC resistor R_1.

electrode, while the Si was held at 0V. In order to reduce Joule heat effect, the current flow through the SiC resistor was set to 5μA. Hence the leakage current was only about 0.05% of the applied current. The IV curve of SiC resistor shows good linearity indicating that the Al has formed a good Ohmic contact to the SiC (Fig. 3, right side).

III. Gauge Factor Measurement

Fig. 4 shows the experimental setup for measuring the gauge factor. Strain was induced by applying the bending beam method. The resistance change of the SiC resistor was measured by the 4 points measurement by using an Agilent 34410A Multimeter. As the thickness of the SiC is much smaller than Si, the strain of SiC induced by bending moment is expected to be the same as that of the upper surface of Si: $\varepsilon = Mt/(E_{Si}I)$, where M is the bending moment, E_{Si} is the Young's modulus in [110] orientation of Si, I is the inertial moment, and t is the thickness of Si beam. The relative resistance changes show a good linear relationship with the applied strains which varied from 0ppm to 800ppm (Fig. 5). The ratios of the relative resistance changes to the normal strains in [110] orientation of SiC resistors with different lengths and orientations are shown in Table I.

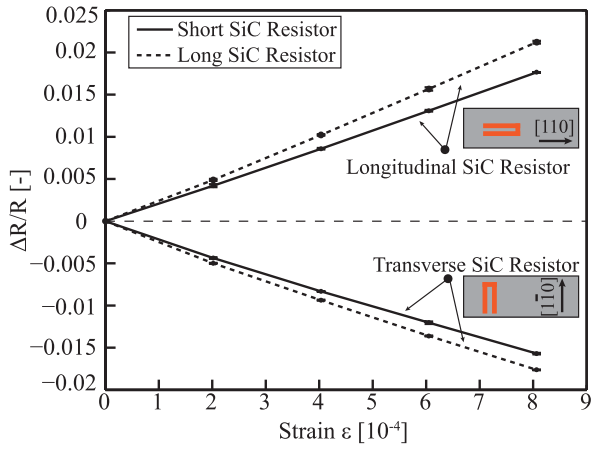

Fig. 5. Response of fractional resistance change of 3C-SiC resistor to applied strain. Longitudinal SiC resistors had positive GFs while transverse SiC resistors had negative GFs.

TABLE I
RATIO OF RESISTANCE CHANGE TO STRAIN OF 3C-SiC RESISTORS

Orientation	[110]		[1$\bar{1}$0]	
Length[μm]	1050	550	1050	550
$(\Delta R/R)/\varepsilon$	25.8	21.6	-22.6	-20.0

The following method is proposed to calculate the longitudinal and transverse GFs. Consider a pair of long and short longitudinal SiC resistors R_L and R_S aligned in [110] orientation (Fig. 4). Each resistor consists of two sections: transverse section R_1 and longitudinal section R_2 (R_1' and R_2' for the short SiC resistor). When a stress is applied in [110] orientation, the resistance change ΔR_1 in section R_1 and $\Delta R_1'$ in section R_1' correspond to the transverse GF, while the resistance changes ΔR_2 in section R_2 and $\Delta R_2'$ in section R_2' correspond to the longitudinal GF. Since the long and short SiC resistors were designed to be in almost the same position, it was assumed that the strains of these two resistors were identical. Hence, the longitudinal gauge factor (GF_L) of p-type 3C-SiC in [110] orientation is deduced as:

$$GF_L = \frac{1}{\varepsilon}\frac{\Delta R_2}{R_2} = \frac{1}{\varepsilon}\frac{\Delta R_2'}{R_2'} = \frac{1}{\varepsilon}\frac{\Delta R_2 - \Delta R_2'}{R_2 - R_2'}$$

As the transverse sections R_1 and R_1' of the long and short SiC resistors were designed to have the same dimensions ($R_1 = R_1'$ and $\Delta R_1 = \Delta R_1'$), hence:

$$\begin{cases} R_2 - R_2' = (R_2 + R_1) - (R_2' + R_1') = R_L - R_S \\ \Delta R_2 - \Delta R_2' = (\Delta R_2 + \Delta R_1) - (\Delta R_2' + \Delta R_1') = \Delta R_L - \Delta R_S \end{cases}$$

Therefore, the longitudinal GF_L in [110] orientation is:

$$GF_L = [(\Delta R_L - \Delta R_S)/(R_L - R_S)]/\varepsilon$$

From above equation, the longitudinal GF_L of p-type 3C-SiC in [110] orientation was calculated to be 30.3. Using the same method, the transverse GF_T of p-type 3C-SiC in [110] orientation was -25.1. These values were larger than the GFs of the p-type polycrystalline 3C-SiC reported in previous research [14]. In addition, the GF of the p-type 3C-SiC presented in this work is comparable with the GF of the p-type 6H-SiC reported by Okojie *et al.* ($GF = 27$) [8], indicating that p-type single crystalline 3C-SiC is a potential candidate for MEMS mechanical sensors.

The longitudinal and transverse GFs were used to calculate the piezoresistive coefficient based on the following equations:

$$\begin{cases} GF_L = E_{SiC}(\pi_{11} + \pi_{12} + \pi_{44})/2 \\ GF_T = E_{SiC}(\pi_{11} + \pi_{12} - \pi_{44})/2 \end{cases}$$

Accordingly, the piezoresistive coefficient π_{44} in the principle coordinate was calculated to be about 16×10^{-11}[Pa^{-1}].

IV. CONCLUSION

The gauge factor and piezoresistive coefficient π_{44} of p-type single crystalline 3C-SiC thin film grown on p-type Si (100) substrate by LPCVD at 1000 °C have been characterized. The high gauge factor up to 30.3 in [110] direction demonstrated the potential applications of p-type 3C-SiC in mechanical-sensors development.

REFERENCES

[1] D. V. Dao, T. Toriyama, and J. Wells, *et al.*, "Silicon piezoresistive six-degree of freedom force-moment micro sensor," *Sensors Mater.*, vol. 15, no. 3, pp. 113–135, 2003.
[2] D. V. Dao, T. Toriyama, and S. Sugiyama, "Noise and frequency analyses of a miniaturized 3-DOF accelerometer utilizing silicon nanowire piezoresistors," in *Proc. IEEE Sensors*, Vienna, Austria, Oct. 2004, pp. 1464–1467.
[3] D. V. Dao, K. Nakamura, and T. T. Bui, *et al.*, "Micro/nano-mechanical sensors and actuators based on SOI-MEMS technology," *Adv. Nat. Sci, Nanosci. Nanotechnol.*, vol. 1, no. 1, p. 013001, 2010.
[4] P. M. Sarro, "Silicon carbide as a new MEMS technology," *Sens. Actuators A, Phys.*, vol. 82, nos. 1–3, pp. 210–218, 2000.
[5] J. Bi, G. Wei, L. Wang, and F. Gao, *et al.*, "Highly sensitive piezoresistance behaviors of n-type 3C-SiC nanowire," *J. Mater. Chem. C*, vol. 1, pp. 4514–4517, Jun. 2013.
[6] T. Akiyama, D. Briand, and N. F. Rooij, "Design-dependent gauge factors of highly doped n-type 4H-SiC piezoresistors," *J. Micromech. Microeng.*, vol. 22, no. 8, p. 085034, 2012.
[7] M. A. Fraga, H. Furlan, and R. S. Pessoa, *et al.*, "Studies on SiC, DLC and TiO_2 thin films as piezoresistive sensor materials for high temperature application," *Microsyst. Technol.*, vol. 18, pp. 1027–1033, Aug. 2012.
[8] R. S. Okojie, A. A. Ned, and A. D. Kurtz, *et al.*, "Characterization of highly doped n and p-type 6H-SiC piezoresistors," *IEEE Trans. Electron Devices*, vol. 45, no. 4, pp. 785–790, Apr. 1998.
[9] M. Mehregany, C. A. Zorman, and N. Rajan, *et al.*, "Silicon carbide MEMS for harsh environments," *Proc. IEEE*, vol. 86, no. 8, pp. 1594–1610, Aug. 1998.
[10] S. J. Shor, D. Goldstein, and A. D. Kurtz, "Characterization of n-type β-SiC as a piezoresistor," *IEEE Trans. Electron Devices*, vol. 40, no. 6, pp. 1093–1099, Jun. 1993.
[11] M. Eickhoff, M. Moller, and G. Kroetz, *et al.*, "Piezoresistive properties of single crystalline, polycrytalline, and nanocrystalline n-type 3C-SiC," *J. Appl. Phys*, vol. 96, no. 5, pp. 2872–2879, 2004.
[12] C. H. Wu, C. A. Zorman, and M. Mehregany, "Fabrication and testing of bulk micromachined silicon carbide piezoresistive pressure sensor for high temperature application," *IEEE Sensors. J.*, vol. 6, no. 2, pp. 316–324, Apr. 2006.
[13] R. Ziermann, J. V. Berg, and E. Obermeier, *et al.*, "High temperature piezoresistive β-SiC-on-SOI pressure sensor with on chip SiC thermistor," *Mat. Sci. Eng. B*, vols. 61–62, no. 1, pp. 576–578, 1999.
[14] T. Homma, K. Kamimura, and H. Y. Cai, *et al.*, "Preparation of polycrystalline SiC films for sensors used at high temperature," *Sens. Actuators A, Phys.*, vol. 40, no. 2, pp. 93–96, 1994.
[15] L. Wang, S. Dimitrijev, and J. S. Han, *et al.*, "Demonstration of p-type 3C-SiC grown on 150 mm Si(100) substrates by atomic-layer epitaxy at 1000 °C," *J. Cryst. Growth*, vol. 329, pp. 67–70, Jan. 2011.
[16] L. Wang, S. Dimitrijev, and G. Walker, *et al.*, "Color chart for SiC thin films grown on Si substrate," *Mater. Sci. Forum*, vols. 740–742, pp. 279–282, Jan. 2013.